Hydrogen Atom Addition to Hydrocarbon Guests in Radiolyzed Zeolites[†]

D. W. Werst,* P. Han, S. C. Choure, E. I. Vinokur, L. Xu, and A. D. Trifunac*

Chemistry Division, Argonne National Laboratory, Argonne, Illinois 60439

L. A. Eriksson*

Department of Quantum Chemistry, Uppsala University, Box 518, S-751 20 Uppsala, Sweden

Received: March 2, 1999; In Final Form: April 25, 1999

The formation of H adducts during radiolysis of zeolites containing olefinic and aromatic hydrocarbon guests was demonstrated to occur by H atom transfer from the zeolite to the adsorbed molecules. The H adducts and other paramagnetic radiolysis products (radical cations and H-loss radicals) were detected by EPR spectroscopy. The mechanism of H adduct formation was confirmed by, inter alia, H/D isotopic labeling and comparison of results in HZSM5 and H−Mordenite to results in their Na$^+$-exchanged counterparts. The effects of charge transfer among radiolysis products and zeolite−adsorbate interactions on the relative yields of trapped species is discussed. It is proposed that molecules smaller that a critical size adsorb inhomogeneously in ZSM5, forming aggregates in which ion−molecule reactions occur. Interpretation of the experimental results was aided by quantum chemical calculations of the molecular properties of the intermediates and their reaction energetics. This included evaluation of electron-transfer exothermicities, activation energies for H addition, and the relative acidities of the radical cations.

1. Introduction

The fundamental understanding of chemistry in heterogeneous systems underpins many critical technologies for energy production, environmental protection, communications, and microelectronics, to name a few. This chemistry is typified by reactions on surfaces, at interfaces, and in constrained spaces. Radiation chemical techniques are well-suited for studying heterogeneous systems, for example, for generating very reactive intermediates whose chemical reactions can be studied under diverse conditions. Furthermore, radiation chemistry is relevant for specific technologies: radiation catalysis is a promising advanced oxidation process (AOP) for environmental remediation;[1−3] electron beam lithography is the focus of efforts to continue the revolution in electronics and optics brought on by miniaturization;[4−6] and radiation effects impact the durability of vitrified waste forms for long-term disposal of high-level nuclear waste.[7]

The radiation chemistry of heterogeneous solids has been much less studied than that of gases and homogeneous solutions. Often the subject of such studies has been a porous solid, such as silica gel and zeolites. Closely related are photochemical studies in heterogeneous solids. Like radiation chemistry, photochemistry often involves charge separation to initiate chemistry. For example, photoinduced electron transfer in zeolites has been explored as a possible way to mimic the ability of natural systems to achieve a bias against back electron transfer.[8−10] It has been shown that zeolite-based photochemistry can exploit the electrostatic fields and geometry constraints inside such specialized microreactors to lower the energy requirements and increase the selectivity of important chemical reactions.[11,12]

In our laboratory we have used zeolites to sequester radical cations and study their reactions under the geometric constraints imposed by the matrix.[13−21] Zeolites and related materials present intriguing possibilities for studying fundamental radiolytic processes in heterogeneous solids. In the first place, they are realistic simulants of minerals and clays in soils and representatives of solid catalysts. Second, ordered solids with variable pore size, acidity, etc., allow the construction, with the inclusion of guest molecules, of idealized model systems for probing primary radiation processes. These include ionization, charge transfer, energy transfer, ion−molecule reactions, electron reactions, and H atom reactions. In addition to understanding these primary processes individually, it is important to understand how they are interrelated in the context of heterogeneous solids.

The radiolysis of hydrocarbons in ZSM5 has been the subject of previous publications from our laboratory where we have specifically discussed reactions of excited radical cations,[14−16] hole transfer,[18] electron reactions,[17] ion−molecule reactions,[16,20,21] and radical cation−adsorbate and radical cation−host interactions.[19] In this paper, we aim to summarize the primary mechanism for radiolysis of hydrocarbons in this zeolite with one key addition: the reactions of radiolytic hydrogen atoms with adsorbate molecules. This picture has been drawn from the vantage point of the radiolysis/EPR method, which allows precise identification of paramagnetic radiolysis products trapped in the zeolite at low temperatures. What has emerged is an increasingly detailed view of a rather specialized system— but one which offers insights into fundamental processes that span many heterogeneous solid environments.

The most common processes that occur in the radiolysis of hydrocarbons in ZSM5 are depicted in eqs 1−4. The choice of isobutene is only for illustration. In all cases, ionization of the guest species occurs by electron transfer to the radiation-induced

matrix holes (Z$^{\bullet+}$), eq 2. Failure to isolate radical cations from unoxidized molecules results in ion–molecule reactions, most typically proton transfer, eq 3. Isolation of radical cations in ZSM5 is achieved only for a narrow range of molecules whose size is closely matched to the size of the ZSM5 channels (ca. 5.5 Å).

(1)

(2)

(3)

(4)
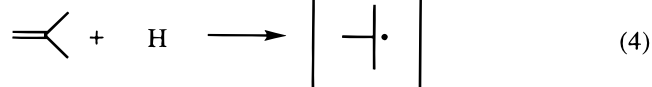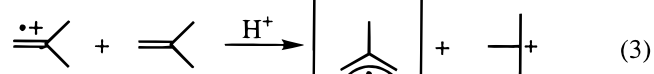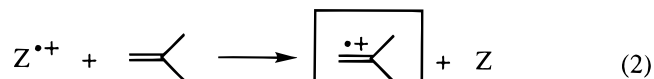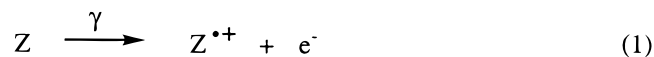
Another process that occurs is the addition of hydrogen atoms to adsorbate molecules to give H adduct radicals, eq 4. For benzene adsorbed on silica gel it was shown that H adducts are formed during radiolysis at 77 K by transfer of H atoms from the matrix to the adsorbed molecules.[22] Activation-controlled addition of H atoms to pyrene was studied on silica gel by transient optical absorption.[23] We and others reported the formation of H adducts during the radiolysis of hydrocarbons in zeolites, but the formation of H adducts was not studied in depth—neither the mechanism nor how it might interact with other reaction channels.[24–27]

The H adduct, the radical cation, and the H-loss radical are the three most typical paramagnetic species that are observed following the low-temperature radiolysis of hydrocarbons in ZSM5 (and related matrixes). The relative contributions of these three species to the EPR spectrum is very dependent on conditions and the choice of matrix and the adsorbate. In ZSM5 it is possible, with the right choice of adsorbate, to eliminate the ion–molecule channel (proton transfer) and focus on the relative yields of trapped radical cation and H adduct. This is the main new information in this paper. Specifically, we examine the mechanism of H adduct formation and possible reasons for the observed variations in the relative contribution of the H adduct to the spectrum of trapped radiolysis products at low temperature.

Interpretation of the radiolysis/EPR results is aided by the theoretical investigation of the structures and properties of the intermediates and their reaction energetics.

2. Experimental Section

2.1. Materials and Methods. Mordenite and ZSM5 zeolites were received from Chemie Uetikon of Switzerland. The siliceous MCM-41 was synthesized according to the method in the literature.[28] The hydrocarbons used were purchased from Aldrich and ChemSampCo.

Zeolite samples were prepared on a glass vacuum manifold in 4 mm o.d. Suprasil sample tubes. The sample tube containing 50 mg zeolite powder (30 mg for MCM-41) was evacuated ($\leq 10^{-4}$ Torr) and heated to approximately 450 °C for 4–6 h. The hydrocarbon liquids were degassed by several freeze–pump–thaw cycles before transferring a quantitative amount to the zeolite powder. Unless otherwise noted, the sealed sample tubes were allowed to equilibrate overnight at room temperature.

The samples were irradiated at 77 K by ^{60}Co γ-rays or by a 3 MeV electron beam at variable temperature. The radiolysis dose was typically between 3 and 5 kGy. *G* values (number per 100 eV absorbed) are not reported below, but the yield of ionized adsorbate can be significant; for example, the radical cation of tetramethylethylene is formed with a G on the order of 1 or slightly greater in ZSM5. EPR spectra (X-band, microwave frequency of 9.3–9.4 GHz) of irradiated samples were collected at temperatures between 4 K and room temperature. Temperature control was achieved with a liquid helium transfer cryostat (APD or Oxford). Normally, data collection was begun at approximately the radiolysis temperature and then the EPR spectrum was repeatedly scanned, for example, at 20° intervals, as the sample was slowly annealed. Any changes in the EPR spectrum were tested for reversibility. The sample was normally not maintained at any given temperature for more than 15–30 min.

2.2. Results. The zeolite ZSM5 is a high silica zeolite with a three-dimensional network of intersecting channels.[29] A system of 5.3 × 5.6 Å straight channels is connected by 5.1 × 5.5 Å sinusoidal channels, with approximately 700 μmol channel intersections per gram of zeolite (4 uc^{-1}). The proton-exchanged form, HZSM5, is a strong Bronsted acid, while NaZSM5 is catalytically inactive. The concentration of Bronsted acid sites ($\equiv$AlO(H)Si$\equiv$), or bridging hydroxyls, is approximately equal to the concentration of aluminum atoms in the zeolite. The SiO$_2$/Al$_2$O$_3$ ratio of ZSM5 is variable and will be denoted where appropriate by a numerical suffix. In the present work experiments were carried out in the following: NaZSM5-170, NaZSM5-210, HZSM5-240, and HZSM5-400. The adsorbates used in our study were unsaturated hydrocarbons—olefins, benzene, and toluene.
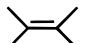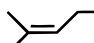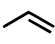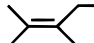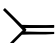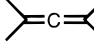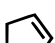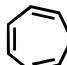
Some results are also reported in Mordenite and MCM-41. Mordenite, like ZSM5, is a channel-type zeolite (6.5 × 7.0 Å channels intersecting 2.6 × 5.7 Å channels).[29] The H–Mordenite had a SiO$_2$/Al$_2$O$_3$ ratio of 25. MCM-41 is an ordered, mesoporous molecular sieve with a hexagonal array of channels.[28] The MCM-41 used by us was the pure silica form which gave a d$_{100}$ peak at approximately 33 Å in the X-ray powder diffraction pattern. This value is taken as the estimate of the pore diameter.

2.2.1. NaZSM5: Trapping Radical Cations. The most prevalent species observed by EPR following radiolysis of unsaturated hydrocarbons in NaZSM5 were the radical cation and the H-loss radical. One species was dominant in the EPR spectrum collected at approximately 77 K after radiolysis in liquid nitrogen; coexistence of the two products was not the norm. Table 1 summarizes these results.

The ability to trap radical cations in NaZSM5 is strongly correlated with adsorbate size. Molecules larger than those in the table adsorb into the ZSM5 channels from the gas phase with difficulty or not at all (and gave correspondingly weak EPR signals). Molecules with fewer than six carbons did not yield trapped radical cations at 77 K, and gave radical cation decay products instead. Typical experiments involved adsorbate concentrations of 100–200 μmol/g. Lowering the adsorbate concentration to as low as 30 μmol/g did not increase the occurrence of trapped radical cations for the entries in the right-hand column of Table 1.

Upon sample annealing, radical cations trapped at 77 K eventually decay, and often the EPR signal of the H-loss radical was observe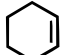d.[16] This is attributed to the onset of diffusion (of neutral molecules) and ion–molecule reactions (proton transfer). The onset temperature for the formation of the H-loss radical

Hydrogen Addition to Hydrocarbons in Radiolyzed Zeolites

J. Phys. Chem. B, Vol. 103, No. 43, 1999 **9221**

TABLE 1. Comparison of Adsorbates for Which Radical Cations Were Observed in NaZSM5 and Those for Which Radical Cations Were Not Observed[a]

radical cation observed	radical cation NOT observed

[a] Paramagnetic decay product observed at 77 K shown in brackets. Previous work is cited.

Figure 1. (a) EPR spectrum of the cyclohexene radical cation (a(2H) = 55.3 G, a(2H) = 23.5 G, a(2H) = 8.5 G) observed at 90 K in NaZSM5 with 350 μmol/g cyclohexene. (b) EPR spectrum of the cyclohexenyl radical (a(2H) = 26.5 G, a(2H) = 14.5 G, a(2H) = 8.5 G, a(H) = 3.5 G) observed at 75 K in NaZSM5 with 500 μmol/g cyclohexene. (c) EPR spectrum of the cyclopentenyl radical (a(4H) = 24.5 G, a(2H) = 14.3 G, a(H) = 3.0 G) observed at 4 K following the 4 K radiolysis of 60 μmol/g cyclopentene in NaZSM5.
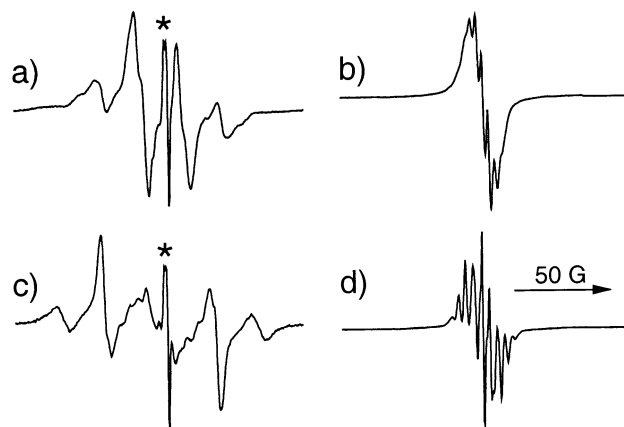
Figure 2. (a) EPR spectrum of ethyl radical observed at 90 K in NaZSM5-210 with 250 μmol/g ethylene. (c) Sample annealing to 190 K caused the conversion of the EPR signal from ethyl to that of the *n*-butyl radical. Corresponding spectra for C_2D_4 are shown in (b) (90 K) and (d) (170 K). The sharp feature marked by asterisks in (a) and (c) is due to defect centers in the suprasil sample cells. This signal is present in all spectra to varying degrees.

can be lowered by increasing the adsorbate concentration. For example, at a loading of 350 μmol/g cyclohexene, the EPR signal from the cyclohexene radical cation persisted up to approximately 120 K (Figure 1a); at higher temperatures the radical cation decayed and was replaced by the cyclohexenyl radical. At a loading of 500 μmol/g cyclohexene, the cyclohexenyl radical was observed at 77 K and no radical cation was present (Figure 1b).

Thus failure to adsorb molecules in an isolated fashion would explain the failure to trap the radical cations of molecules with fewer than six carbons. As a further test, we irradiated isobutene and cyclopentene in NaZSM5 at 4 K. The results were the same as for 77 K radiolysis: signals from the H-loss radicals, 2-methylallyl and cyclopentenyl, dominated the EPR spectra. The cyclopentene result is shown in Figure 1c. Without doubt, deprotonation of the radical cations occurs without diffusion at 4 K. We believe the same is true at 77 K.

The radiolysis/EPR results for ethylene—the only adsorbate to give rise to the H adduct product in NaZSM5—are presented in Figure 2. The ethyl radical can be assigned by the similarity of the EPR spectrum in Figure 2a to the ethyl radical EPR spectrum generated by radiolysis of ethyliodide on silica gel.[32] In NaZSM5 the line width is greater which, together with hyperfine anisotropy, makes the estimation of the quartet and triplet hyperfine coupling constants more difficult. They are on the order of 25 and 20 G, respectively.

Tellingly, the initial product observed after radiolysis of ethylene-d_4 on NaZSM5 was $C_2D_5{}^\bullet$ (Figure 2b). This demonstrates conclusively that the hydrogen atom is not donated by the matrix, in which case the product would be $HCD_2CD_2{}^\bullet$ and the EPR spectrum would exhibit a doublet splitting on the order

of 25 G. The ratio a(H)/a(D) for ethyl radical in NaZSM5 appears to be approximately 7, compared to about 6.5 for the isotropic coupling constants in solution.[33] We argue in Section 4 that the ethyl radical results from ionization of ethylene followed by the reaction of ethylene radical cation with ethylene.

Upon annealing the ethylene/NaZSM5 sample, the ethyl radical decayed and a new EPR signal grew in, a process that began at about 140 K and was complete by 170−190 K (Figure 2c). The new spectrum resembles that of the *n*-butyl radical, which was previously reported in argon,[34,35] SF_6,[36] and ZSM5
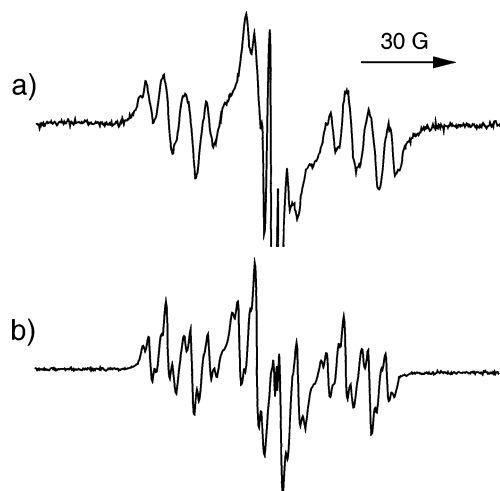
Figure 3. (a) EPR spectrum of cyclohexadienyl radical observed at 75 K in MCM-41 with 120 μmol/g 1,4-cyclohexadiene. (b) EPR spectrum of the cyclohexadienyl radical (a(2H) = 48 G, a(H) = 13 G, a(2H) = 9 G, a(2H) = 2.6 G) observed at 135 K in a frozen solution of 20 μmol/g 1,4-cyclohexadiene in perfluoromethylcyclohexane.

matrixes.[37] At low temperature the two β-proton couplings are not equivalent. One coupling constant is nearly equal to the isotropic coupling constant for the α-protons (22 G) and the second is in the range 38−47 G, depending on matrix and temperature. In our ethylene/NaZSM5 sample, this coupling constant varied from 47 G at 4 K to approximately 38 G at 190 K. Anisotropy, particularly in the hyperfine coupling to the α-protons, accounts for the broadening of the spectrum. A nearly identical spectrum was generated by radiolysis of 1-iodobutane in NaZSM5. The thermal transformation observed for C_2D_4 mirrored that of the C_2H_4-loaded zeolite (Figure 2d).

The thermal transformation of ethyl radicals into *n*-butyl radicals is assumed to take place by radical addition to ethylene. A longer, chain-end radical would be difficult to distinguish from the *n*-butyl radical and therefore we cannot rule out the possibility that higher polymers are formed. For the sake of discussion, we will refer to this propagating radical as *n*-butyl.

Observation of radical cations was less successful in a silica matrix with larger pore diameter. In MCM-41, the radical cations of benzene and tetramethylethylene (TME) were observed (these formed dimer radical cations at higher loadings), but when 1,3,5-cycloheptatriene, cyclohexadiene, norbornadiene, and cyclohexene were tested in MCM-41 they gave predominantly the H-loss radicals at 77 K. Figure 3 shows the result for 120 μmol/g 1,4-cyclohexadiene. The EPR spectrum of cyclohexadienyl radical in MCM-41 is compared to the spectrum observed at 135 K in a frozen solution of 20 μmol/g 1,4-cyclohexadiene in perfluoromethylcyclohexane. In the latter case, the H-loss radical was formed by ion−molecule reaction of the 1,4-cyclohexadiene radical cation (stable below 120 K) upon annealing the sample above the softening point of the matrix (approximately 125 K).

Decreasing the adsorbate concentration in MCM-41 did not increase the occurrence of trapped radical cations. For example, 1,3,5-cycloheptatriene gave approximately 85% tropyl radical (a(7H) = 4 G)[38] and 15% radical cation (a(2H) = 51 G, a(4H) = 5 G)[39] at a loading of 120 μmol/g. The relative contribution of the radical cation did not increase when the loading was decreased to as low as 10 μmol/g.

2.2.2. HZSM5: H Adducts. HZSM5 is a strong Bronsted acid and without care catalytic transformations of the hydrocarbon adsorbates can intrude on the study of radiolytic

TABLE 2. Adsorbates Tested in HZSM5[a]
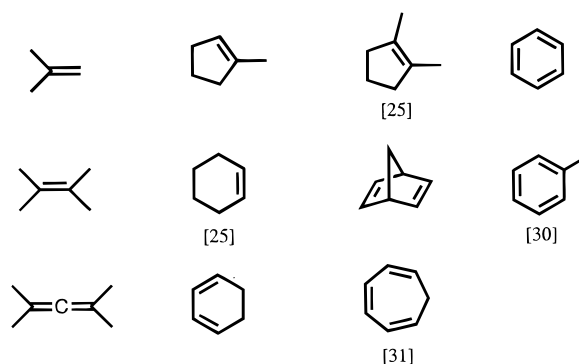
[a] Previous work is cited.

TABLE 3. Isotropic Proton Hyperfine Coupling Constants (*G*; 1 *G* = 0.1 mT) for H Adduct Radicals in HZSM5[a]

radical	adsorbate	T(K)	a(CH$_3$)	a(CH$_2$)	a(CH)
	isobutene	90	22.4 (21.2)		
	1-methylcyclopentene	90	23.5 (21.8)	24.5 (23.2) 44.0 (41.1)	
	tetramethylethylene	210	23.0 (21.4)		5.2 (5.7)
	tetramethylallene	130	14.5 (14.0) 13.5 (12.8)		4 (5.3)
	benzene	150		48 (49.6)	13 (-12.3) 9.0 (-9.4) 2.6 (3.5)

[a] Computed results (B3LYP/6-311G(2df,p)) in parentheses.
[a] Computed results (B3LYP/6-311G(2df,p)) in parentheses.

processes in this zeolite. We have shown that the radiolysis/EPR method can be used effectively to elucidate such catalytic processes and to distinguish between the catalytic effects and genuine radiation chemistry.[24,25] Under the conditions of the experiments reported in this study, catalytic reactions of the adsorbates were minimized or in most cases excluded.

A new feature in the radiolysis/EPR results in HZSM5, compared to NaZSM5, was the appearance and, in a few cases, the dominance of the signal from the H adduct. The H adducts were formed during radiolysis; they were not formed by thermal reactions after radiolysis. Table 2 lists the adsorbates tested in HZSM5, and Table 3 lists hyperfine coupling constants for H adduct radicals. Smaller molecules (<C$_6$) were omitted for the most part because the goal was to measure the relative yields of radical cation and H adduct without the loss of radical cation by deprotonation. In addition, the smaller olefins undergo more rapid catalytic reactions (dimerization, etc.) on HZSM5 at room temperature. For larger olefins (>C$_5$), this was not a problem. Isobutene was equilibrated on HZSM5 at subambient temperature (225 K) for only 5 h to limit loss of monomeric starting material due to acid-catalyzed reactions.

A caveat that must be made here is that different species in an EPR spectrum are not detected with equal sensitivity. Spectral overlap can cause a minor species to be masked by a more dominant signal. Second, EPR detection sensitivity decreases with increasing number of spectral lines and line width. With this in mind, we proceed with due caution to discuss the radiolysis/EPR results in HZSM5.
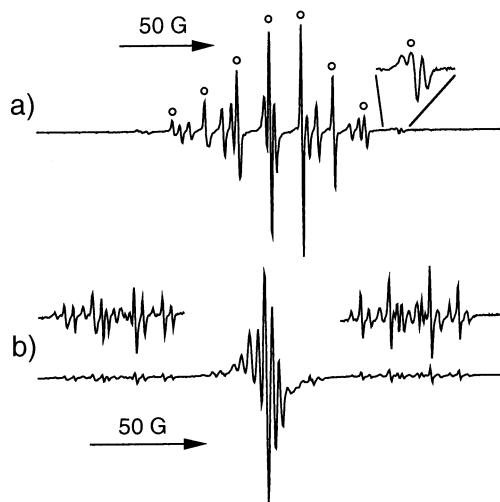
Hydrogen Addition to Hydrocarbons in Radiolyzed Zeolites

J. Phys. Chem. B, Vol. 103, No. 43, 1999 **9223**

Figure 4. (a) EPR spectrum observed at 205 K in HZSM5-400 with 120 μmol/g TME. The radical cation lines are labeled with open circles. All other lines belong to the tetramethylethyl radical. (b) EPR spectrum observed at 150 K in HZSM5-240 with 150 μmol/g benzene. The outer portions of the cyclohexadienyl spectrum are expanded in the upper trace.

The two most optimal cases for quantitating the relative yields of radical cation and H adduct were TME and benzene (Figure 4). The TME radical cation signal (a(12H) = 17.1 G) is well-resolved from the EPR spectrum of the H adduct, tetramethylethyl. The contributions of the two species to the EPR spectrum in Figure 4a, estimated by spectral simulation, are approximately equal. This was quite reproducible for constant loading and sample equilibration conditions.

Benzene on HZSM5 gave rise to both monomer (a(6H) = 4.5 G) and dimer radical cations (a(12H) = 2.2 G) and the H adduct, cyclohexadienyl (Figure 4b). (The relative contributions of monomer and dimer radical cations were temperature dependent. Above 120 K monomer radical cations reacted with neighboring molecules to form dimer radical cations. Interestingly, this process is hindered in HZSM5 by increasing the concentration of ≡AlO(H)Si≡ groups and is stopped altogether on NaZSM5-210. Benzene diffusion in ZSM5 is apparently acutely sensitive to the channel modifications caused by aluminum substitution in the lattice and ion exchange.) Because the span of the EPR spectrum of the benzene radical cations is much less than that of cyclohexadienyl, it is possible to double integrate the outer portions of the cyclohexadienyl spectrum, multiply by the appropriate factor, and subtract the result from the total spectrum intensity to arrive at the relative yields of radical cations and H adduct. In the example shown in Figure 4b the cyclohexadienyl intensity is approximately 20% of the total, although this was more variable from sample to sample than in the case of TME.

TME was singled out for two additional tests. The ratio of H adduct to radical cation increased with increasing TME concentration (at least 1 order of magnitude between 10 and 120 μmol/g). Second, the ratio of H adduct to radical cation was measured for three different irradiation temperatures: 4, 77, and 170 K. The ratio was constant for 4 and 77 K irradiation but increased by a factor of 2.5 at 170 K.

To summarize the results in HZSM5 for all of the molecules in Table 2, the finding in the majority of cases was a strong contribution from the radical cation (as expected from the discussion of Section 2.2.1). More EPR spectra can be found in the citations given in Table 2. In some cases the spectral
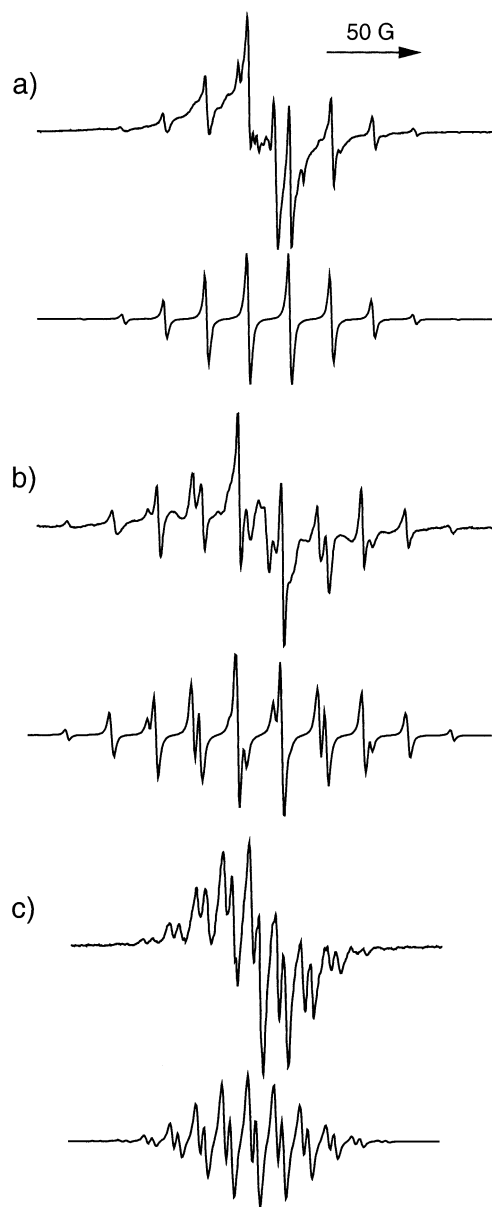
Figure 5. EPR spectra of H adduct radicals formed during 77 K radiolysis of adsorbates in HZSM5 (observation temperatures in parentheses): (a) 120 μmol/g isobutene in HZSM5-240 (85 K), (b) 120 μmol/g 1-methylcyclopentene in HZSM5-240 (85 K), (c) 200 μmol/g TMA in HZSM5-400 (155 K). Each spectrum is accompanied by an isotropic simulation (lower curve) of the H adduct. H adduct structures and coupling constants are given in Table 3.

resolution mitigated against clear identification of the H adduct, but cogeneration of the radical cation and H adduct seems to be the norm. Three cases will be examined more closely because the radical cation was *not* apparent in the EPR spectrum.

The H adduct was very prominent in the result for isobutene (Figure 5a). The radical cation is not expected to be stable; the 2-methylallyl radical is the expected product of ionization of isobutene (vide supra). Unfortunately, even at the low temperature at which this sample was equilibrated, isobutene undergoes some acid-catalyzed reaction.[24] It is possible that overlapping signals from ionized catalysis products and 2-methylallyl account for the spectral components underlying the *tert*-butyl signal. Clear identification of the 2-methylallyl radical was not possible. The prominence of the *tert*-butyl radical signal in this spectrum is aided by the fact that it has only 10 lines and they are very narrow.
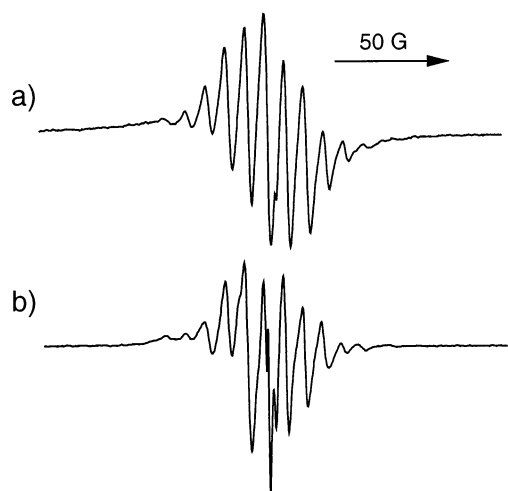
Figure 6. (a) EPR spectrum of the TMA radical cation (a(8H) = 8.4 G) observed at 110 K in a frozen solution of 10 μmol/g TMA in $CF_2ClCFCl_2$. (b) EPR spectrum of the TMA radical cation (a(8H) = 8.3 G) observed at 165 K in NaZSM5-170 with 120 μmol/g TMA.

A second adsorbate for which the H adduct was the major and only identifiable component in the EPR spectrum was 1-methylcyclopentene (Figure 5b). Comparison to the simulated spectrum of the H adduct allows identification of regions of the experimental spectrum where residual signals from an additional species are present. It is impossible to analyze this residual component. Attempts to generate the EPR spectrum of the 1-methylcyclopentene radical cation in NaZSM5 gave a very poor result, as if adsorption was quite limited. Reported EPR spectra of the radical cation in Freon matrixes[40] and our own experimental results in perfluoromethylcyclohexane[41] show that the hyperfine couplings are quite matrix dependent. Therefore direct comparison of these spectra to the spectrum in HZSM5 is problematic. The radical cation spectrum is, at any rate, of considerable width (approximately 230 G) and a signal from a low-to-moderate concentration of this species could be hidden under the strong H adduct signal. A second H adduct isomer is possible for this adsorbate (and others); however, H addition to the less substituted carbon is usually favored and a contribution from a second H adduct could not be verified in this or any other case.

Finally, the result for tetramethylallene (TMA) in HZSM5 is shown in Figure 5c. The dominant signal is due to the H adduct (hyperfine couplings analyzed as in Table 3). For reference the EPR spectrum of TMA[•+] is shown in a Freon matrix and in NaZSM5 (a(12H) = 8.3 G) in Figure 6. From simulations, it can be estimated that the contribution of the radical cation to the experimental EPR spectrum in HZSM5 must be less than 10% (similarly for HZSM5-400 and HZSM5-240). TMA was tested in HZSM5 over a wide concentration range (10−200 μmol/g). The intensity of the H adduct signal increased with loading (constant irradiation dose) and was the dominant signal over the entire concentration range, as it was for radiolysis temperatures of 4, 77, and 170 K.

2.2.3. Isotopic Labeling: C_6D_6. The absence of H adducts in NaZSM5 (excepting the case of ethylene) and their appearance in HZSM5 is strong evidence that the H adducts are formed when H atoms released from the matrix during radiolysis add to the adsorbate. We used isotopic labeling to demonstrate this more directly. Initial efforts using TME, isobutene, and TMA on DZSM5 failed because H/D exchange between the hydrocarbon and deuterated zeolite caused scrambling of the label prior to radiolysis. Benzene, on the other hand, undergoes very
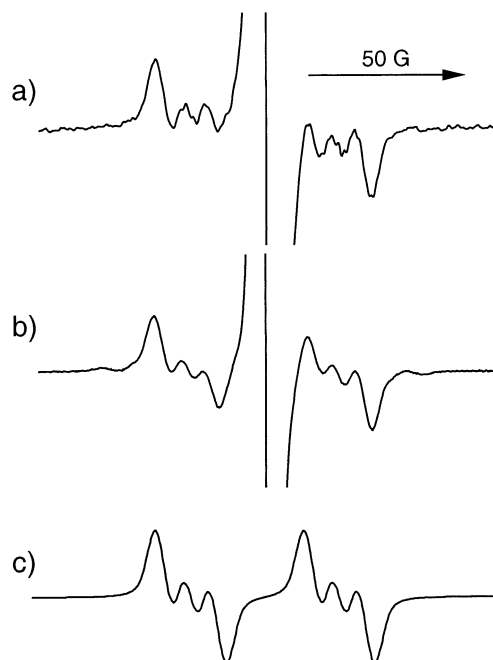
Figure 7. (a) EPR spectrum observed at 90 K in HZSM5-400 with 150 μmol/g benene-d_6. (b) EPR spectrum observed at 90 K in H−Mordenite with 300 μmol/g benzene-d_6. (c) Simulated spectrum of $C_6D_6H^\bullet$.

slow H/D exchange in HZSM5 at room temperature[30,42] and results for benzene-d_6 on HZSM5 and H−Mordenite are shown in Figure 7.

A theoretical EPR spectrum of $C_6D_6H^\bullet$, that is, the cyclohexadienyl radical with one proton, was calculated assuming a(H)/a(D) = 6.0 (Figure 7c). The excellent agreement with experiment confirms that the H adduct in both HZSM5 and H−Mordenite is formed by transfer of a hydrogen atom from the zeolite. (No cyclohexadienyl radical was observed following radiolysis of benzene in Na−Mordenite.) A similar spectrum was reported for benzene-d_6 on silica gel.[22] There is a small additional signal in the wings of the H−Mordenite spectrum that does not belong to $C_6D_6H^\bullet$. This signal increased relative to the other lines with increased contact time between the benzene-d_6 and the zeolite at room temperature prior to radiolysis and is probably due to some cyclohexadienyl radical with more than one proton due to H/D exchange. To minimize this interference the spectra in Figure 7, parts a and b, were collected after only 15 min equilibration at room temperature.

2.2.4. Charge Transfer. In the matrix-isolation experiment one observes what is trapped on the long time scale. A serious question is always whether the relative concentrations of trapped species accurately reflect the relative initial yields, or if some process selectively removes certain species from our observation? A particular concern in matrix-isolation studies of charged species is charge transfer. In the present study, charge transfer from the radical cation to the H adduct is exothermic in all cases (Section 3). This reaction removes two paramagnetic species, eq 5.
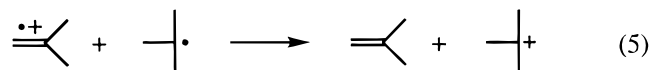
Direct evidence of the formation and parallel decay of the radical cation and H adduct would require a time-resolved experiment, but the possibility of radical cation scavenging by a neutral radical was tested in two variations of the radiolysis/EPR

Figure 8. (a) EPR spectrum of irradiated NaZSM5-210. (b) EPR spectrum of sample in (a) 140 min after addition of 250 μmol/g ethylene. (c) EPR spectrum of 30 μmol/g benzene in NaZSM5-210. (d) EPR spectrum of sample in (c) 11 min after addition of 250 μmol/g ethylene. The observation temperature was 170 K in all cases. The intensity scale is not constant in (a)−(d).
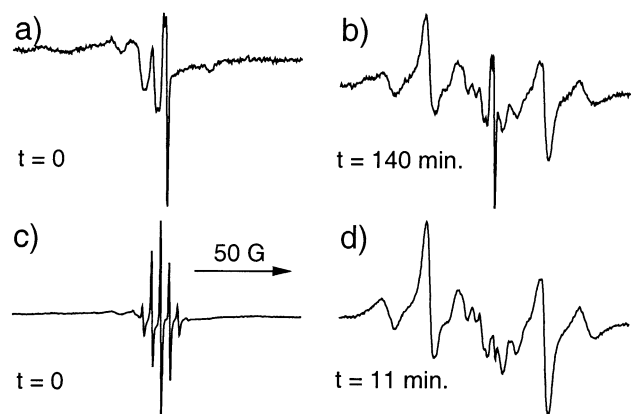
experiment. One variation involved radiolysis of a mixed sample (two adsorbates), and a second involved sequential ionization of two adsorbates.

The sequential ionization of adsorbates depended on the ability to ionize a molecule adsorbed *after* radiolysis of the zeolite. This was first demonstrated for the post radiolysis exposure of NaZSM5 to ethylene. The EPR spectrum of the zeolite irradiated at 77 K (Figure 8a) shows characteristic hyperfine structure due to oxygen hole center-type defects created by radiolysis ($Z^{\bullet+}$ in eq 1).[43] The irradiated zeolite was subsequently dosed with 250 μmol/g ethylene (delivered via a glass vacuum manifold) at 170 K and the EPR spectrum was repeatedly scanned at 170 K. Over time, the "$Z^{\bullet+}$" signal was gradually quenched, and the signal from *n*-butyl radical grew in (Figure 8b).

This experiment demonstrates that persistent hole centers in the zeolite are capable of ionizing molecules introduced after radiolysis. The *n*-butyl radical is the expected product of ethylene ionization in NaZSM5 at 170 K (vide supra).

The above experiment was repeated with benzene loaded (30 μmol/g, overnight equilibration at room temperature) in the NaZSM5 sample before radiolysis. Radiolysis produced the benzene radical cation, but not all of the $Z^{\bullet+}$ was scavenged by benzene (Figure 8c). In less than two minutes after addition of 250 μmol/g ethylene to this sample at 170 K, the benzene radical cation disappeared and was replaced by *n*-butyl (Figure 8d). We attribute this transformation to scavenging of benzene radical cation by *n*-butyl radical (IP = 8.02 eV), and/or its precursor, $C_2H_5^{\bullet}$ (IP = 8.13 eV), produced upon ionization of ethylene. This conclusion is based on the fact that benzene radical cation does not react with ethylene itself. Under conditions where ethylene was not ionized—longer equilibration of benzene prior to irradiation or increased benzene loading (120 μmol/g) led to full scavenging of $Z^{\bullet+}$—the benzene radical cation was stable against the addition of ethylene and no *n*-butyl signal developed.

The sequential experiment was carried out under dynamic conditions (170 K), but for nondiffusing reactants at 77 K the extent of charge transfer depends on the spatial distribution of donor and acceptor. For a test under static conditions a mixture of benzene (60 μmol/g) plus ethylene (120 μmol/g) in NaZSM5 was irradiated at 77 K. No benzene radical cation was observed.

3. Theoretical Results

3.1. Method. All systems were geometry optimized at the hybrid Hartree−Fock−Density Functional Theory level B3LYP/

TABLE 4. Calculated Vertical Ionization Potentials (eV) and Adiabatic Ionization Potentials (italics), Including Zero Point Energy, of Adsorbate Molecules and the Respective H Adducts[a]

	parent	H adduct	ΔIP	ΔE
ethylene	10.54 (10.51) *10.23*	8.54 (8.13) *8.19*	2.00 (2.38)	2.04
isobutene	9.23 (9.24) *8.88*	7.11 (6.70) *6.78*	2.12 (2.54)	2.10
benzene	9.21 (9.25) *9.00*	6.71 *6.67*	2.50	2.33
cyclohexene	8.92 (8.95) *8.55*	7.40 *6.98*	1.52	1.57
toluene	8.75 (8.82) *8.54*	6.46 *6.34*	2.29	2.20
1-methylcyclopentene	8.52 (8.55) *8.19*	6.77 *6.51*	1.75	1.68
tetramethylallene	8.45 (8.5) *7.88*	6.34 *6.26*	2.11	1.62
norbornadiene	8.38 (8.35) *8.01*	7.26 *6.57*	1.12	1.44
tetramethylethylene	8.29 (8.27) *7.87*	6.92 *6.51*	1.37	1.36
1,2-dimethylcyclopentene	8.14 *7.82*	6.67 *6.40*	1.47	1.41
1,3,5-cycloheptatriene	8.13 (8.29) *7.67*	6.92 *6.89*	1.21	0.78
1,3-cyclohexadiene	8.05 (8.25) *7.79*	7.01 *6.92*	1.04	0.87

[a] Experimental values, from ref 53, are in parentheses. [b] ΔE refers to the relaxed (adiabatic) energetics of charge transfer, eq 5.

6-31G(d,p),[44−49] followed by single point energy and property calculations using the larger 6-311G(2df,p) basis set. Frequency calculations were performed at the B3LYP/6-31G(d,p) level, to confirm the correct number of imaginary frequencies. The zero-point energies from the frequency calculations were added to the higher level energetics in all cases (reactions, relative stabilities), except when discussing the vertical ionization potentials. All calculations were carried out using the Gaussian 94 and Gaussian 98 program suites.[50,51]

In the calculations, we did not include any part of the surrounding zeolite, but focused on calculations in a vacuum. The rationale for this was to discover whether the differences in observed behavior can be attributed to the fundamental properties of the hydrocarbons in question, or if a full explanation requires a detailed description of the interactions with the zeolite.

3.2. Charge Transfer. The difference in ionization potentials of the adsorbate and its H adduct is a measure of the driving force for charge-transfer reactions such as that illustrated in eq 5. Vertical and adiabatic ionization potentials were calculated for adsorbate molecules and their H adducts (Table 4). As seen from the table, the agreement between theoretical and experimental ionization potentials are in almost all cases within 1 kcal/mol (0.04 eV). This agrees well with previous findings.[52]

In Table 4 we also list the ZPE-corrected total energies of the charge-transfer reactants vs products as outlined in eq 5, that is, the difference in adiabatic ionization potentials. As expected, all the charge transfer reactions are exothermic, by between 0.8 and 2.3 eV (1 eV = 23 kcal/mol), and the overall energetics closely follow the differences in vertical ionization potentials.

3.3. H Atom Addition. We computed the reaction profiles for H addition to each of the eleven molecules in Table 2 to assess the variation in activation energies in the gas phase. To validate that the correct H adduct products were obtained, the isotropic hyperfine coupling constants were computed at the single point B3LYP/6-311G(2df,p) level, and are compared with

TABLE 5. Energetics (including ZPE) for H-Addition Reactions to the Adsorbates Listed[a]

adsorbate	energy	transition state	H adduct
benzene	−232.320856	+3.65	−21.73
toluene	−271.650065	+2.83	−23.24
1,2-dimethylcyclopentene	−274.051456	+2.28	−31.81
tetramethylallene	−274.018449	+2.02	−54.39
cyclohexene	−234.721116	+1.90	−33.57
tetramethylethylene	−235.932286	+1.45	−34.02
1-methylcyclopentene	−234.720806	+0.73	−34.83
norbornadiene	−271.559287	+0.17	−44.07
1,3-cyclohexadiene	−233.492330	+0.13	−47.64
isobutene	−157.280228	+0.02	−37.04
1,3,5-cycloheptatriene	−271.594416	−0.05	−48.92

[a] All energies are from B3LYP/6-311G(2df,p) calculations on B3LYP/6-31G(d,p) optimized structures. Absolute energies of adsorbates (without hydrogen atom included) are in au; energies for transition states and products are relative to adsorbate + H atom, in kcal/mol. Atomic energy for hydrogen is −0.502156 au at present level of theory.

the experimental data in Table 3. The data displays the normal deviations between theory and experiment known for this method,[54−56] and we may hence conclude that (i) we are investigating the appropriate H adduct systems, and (ii) the influence from the zeolite matrix on the hyperfine coupling constants is minor.

In Table 5 we list the energetics for the H-addition reactions after correction for zero-point vibrational energy. In the case of multiple addition sites, we considered only those generating the most stable products. For all systems the barriers to H addition are very small, between 0 and 4 kcal/mol. We also note that the well-known deficiency of DFT methods, to yield slightly too small reaction barriers,[57,58] is manifested in the negative value obtained for 1,3,5-cycloheptatriene (note, however, that the energetics reported are single point energies on the B3LYP/6-31G(d,p) optimized structures). The largest activation energy, 3.65 kcal/mol, was determined for benzene. This value compares well with the experimental values of 4.30 kcal/mol[59] and 4.56 kcal/mol[60] in the gas phase and in aqueous solutions, respectively. The error in energy barriers should in all cases be well within a few kilocalories per mole.

A general observation is that species that attain a highly localized H adduct radical (tetramethylethylene, isobutene, 1-methylcyclopentene, 1,2-dimethylcyclopentene, and cyclohexene) are all of intermediate stability (32−37 kcal/mol below the isolated reactants). The remaining systems are either less stable (radical extended over 5 sp[2] carbons; benzene and toluene) or more stable (radical extended over 3 sp[2] carbons in allylic fashion) by ca. 10 kcal/mol relative to these.

3.4. Proton Transfer. The stability of radical cations in NaZSM5 toward deprotonation is found to be dependent on the size of the adsorbate. In Section 4 we discuss the interpretation of this size dependence: Is the occurrence of trapped radical cations governed by geometric factors (i.e., matrix−adsorbate interactions and their influence on the adsorbate distribution) or by the thermodynamic stability of the radical cations? To further illuminate this discussion, we optimized geometries and computed single point energies for this set of systems, and thus evaluated the ZPE-corrected proton affinities as $E_{PA} = E(R^{\bullet}) - E(RH^{\bullet+}) + E(H^+)$, where $E(R^{\bullet})$ is the ZPE-corrected absolute energy of the H-loss radical. These are listed in Table 6 and compared with the available gas-phase values. We note similar trends between the experimental and calculated proton affinities of the different H-loss radicals. The larger the system, the greater the proton affinity (the more stable the radical cation against deprotonation). Again, these sets of data are well in line with

TABLE 6. Computed ZPE-Corrected Proton Affinities of the H-Loss Radicals and Experimental Values (Refs 53,61) for $E_{PA} = \Delta H_f(R^{\bullet}) - \Delta H_f(RH^{\bullet+}) + \Delta H_f(H^+)$[a]

RH	calculated	experimental
ethene	185.4	182
propene	180.7	177
isobutene	194.6	194
cyclopentene	195.5	187
cyclohexene	196.2	
1,3-cyclohexadiene	205.0	196
norbornadiene	234.0	
tetramethylethylene	214.7	200
benzene	216.7	211
toluene	203.9	198
1,3,5-cycloheptatriene	204.3	195
tetramethylallene	218.9	

[a] All energies are in kcal/mol.

the findings by, for example, Becke (using a slightly different functional).[52]

4. Discussion

The reactions of H atoms at cryogenic temperatures have been studied extensively, and it is known that hydrogen addition to unsaturated hydrocarbons occurs at 77 K or below.[22,32,62−65] At cryogenic temperatures the H addition reaction is controlled primarily by H atom diffusion. Diffusion control of this reaction is in accordance with (1) negligible activation energies in some cases (Table 5) and (2) the occurrence of quantum mechanical tunneling of H atoms when the reaction is not barrier-free.

The scission of lattice O−H bonds (silanols or bridging hydroxyls) provides a source of H atoms in the radiolysis of silicates. In pure silica radiolytic O−H scission occurs via trapping of excitons;[23,66] in aluminosilicates a possible alternative mechanism is the electron reaction with acidic protons.

Transfer of lattice hydrogen to the adsorbate, however, is not the only possible mechanism of H adduct formation. Homolytic scission of C−H bonds has been reported, for example, during radiolysis of hydrocarbons adsorbed on Vycor glass[67] and in a xenon matrix.[63] Radiolysis of ethylene in a xenon matrix at 4 K gave rise to vinyl radicals and trapped H atoms that, upon annealing to 45 K, reacted to give ethyl radicals. Thus the signature of the homolytic mechanism is the formation of two radicals.

Radiolysis of ethylene in NaZSM5 at 77 K gives ethyl radical alone—homolysis can be ruled out. The observation of the $C_2D_5^{\bullet}$ product for deuterated ethylene in NaZSM5 excludes H atom transfer from the matrix. We conclude that ethyl radical is the product of an ion−molecule reaction, the nature of which is still speculative. In the gas-phase, ion−molecule reactions proceed via cluster ion intermediates, $(C_2H_4)_n^{\bullet+}$, and product ions are observed with two, three, and four carbons.[68,69] Dissociation of $(C_2H_4)_n^{\bullet+}$ in the zeolite to give $H + C_4H_7^+$ could lead to ethyl radical in ZSM5 by H addition to ethylene; alternatively, ethyl radical may be produced directly by dissociation to give $C_2H_5^{\bullet} + C_2H_3^+$.

Finally, the radiolysis of neat benzene gives rise to cyclohexadienyl radicals.[33,70,71] While there is evidence of a second radical formed, conclusive identification of the phenyl radical has not been possible. Therefore, whether cyclohexadienyl forms by ion−molecule reaction or homolysis seems open to question.

The above considerations raise the burden of proof for assigning the mechanism for formation of H adducts in zeolite radiolysis. Is there one mechanism or more than one? Can radical cations be precursors of H adducts? How can one explain

Hydrogen Addition to Hydrocarbons in Radiolyzed Zeolites

J. Phys. Chem. B, Vol. 103, No. 43, 1999 **9227**

a very weak contribution from the radical cation? We assess the evidence below.

4.1. Mechanism of H Adduct Formation. In HZSM5 and H−Mordenite, tests with benzene-d_6 clearly show that the cyclohexadienyl radical is formed by H atom transfer from the zeolite to benzene. Despite not being able to accomplish the isotopic labeling experiment for olefins in HZSM5 because of exchange, we conclude that benzene is representative and that H atom transfer from the zeolite to adsorbates occurs generally in proton-exchanged ZSM5. Several arguments support this conclusion.

Our quantum calculations show that all other adsorbate molecules tested in HZSM5 have a smaller activation energy for H addition than benzene. If H atoms add to benzene, then there is no energetic reason for addition to the other adsorbates not occurring as well.

Simple removal of bridging hydroxyl groups (where adsorbed olefins and aromatic hydrocarbons tend to be sited because of hydrogen bonding interactions) by cation exchange all but eliminates the contribution from H adducts.[72] The only exceptional case in NaZSM5—ethylene—involves the generation of the H adduct by an ion−molecule reaction, not H atom transfer from the zeolite.

Apart from the unique case of ethylene, however, generation of H adducts by ion−molecule reactions can be ruled out. Naturally, an ion−molecule mechanism fails to explain the dichotomy between NaZSM5 and HZSM5. Furthermore, the H-loss radical is the characteristic product of ion−molecule reactions of olefin radical cations, both in NaZSM5 and in Freon matrixes.[73−75] There are no precedents for H adduct products of condensed-phase ion−molecule reactions involving the olefin molecules used in this study. Finally, except for isobutene, the test molecules in Table 2 were chosen because their radical cations are unreactive when isolated in NaZSM5.

As we have demonstrated, some of the C_6 and C_7 radical cations can react at 77 K to give H-loss radicals, presumably when in contact with another adsorbate molecule. Thus cyclohexene at a high loading of 500 μmol/g gave only cyclohexenyl radical in NaZSM5. A similar concentration dependence for radical cation deprotonation was found for n-alkanes in NaZSM5 at 4 K.[37] Several C_6 and C_7 radical cations gave H-loss radicals at 77 K in MCM-41, where the large pore diameter presents no hindrance to adsorbate aggregation. The alternative explanation, that proton transfer occurs from the radical cation to the matrix (that is, proximity of a second adsorbate molecule is not necessary), requires that MCM-41 is a stronger base than NaZSM5, which seems implausible.

In the case of 1,3,5-cycloheptatriene in MCM-41, although most of the radical cation was converted to the H-loss radical, a fraction survived. This can be understood if a small fraction of the adsorbate is not aggregated and this isolated fraction gives rise to isolated, and thus unreactive, radical cations. If proton transfer to the matrix occurred, then decay of the radical cation would be expected to be complete.[76]

Thus generation of H adducts by ion−molecule reaction in HZSM5 during radiolysis at 77 K is also inconsistent with the expectation that the radical cations of the C_6 and C_7 radical cations are isolated from other adsorbate molecules.

In a related experiment, Roduner et al. used a nonradiolytic technique to ionize TME in HZSM5 and observed TME•+ but no H adduct radical.[78] The nonradiolytic ionization technique entails electron transfer from adsorbate molecules to acceptor sites generated in the zeolite by preactivation in an oxygen atmosphere at high temperature. The conditions of the experiment were somewhat different than ours, but the absence of an H adduct EPR signal is consistent with the conclusion that the H adduct is not formed by ion−molecule reaction.

We therefore rule out an ion−molecule mechanism for producing the H adducts in ZSM5; excepting the case of ethylene, radical cations are not precursors of H adduct radicals. Cogeneration of H adducts and H-loss radicals, signifying C−H bond homolysis, was not observed. We conclude that H adducts are formed by H atom transfer from the HZSM5 to adsorbates during radiolysis.

4.2. Yields of Trapped Species. From our limited survey, and despite the cited difficulties in quantifying the relative radical cation and H adduct yields, it is evident that the H adduct can be the minority species or the majority species with considerable variation for different adsorbates. Below, we consider factors that might affect the H adduct yield, but our first quandary is how to account for the near exclusion in one case (TMA), if not more, of the radical cation signal. Could it be that the formation of H adducts suppresses the yield of trapped radical cations?

It was this question that led us to ponder the net effect of charge transfer from trapped radical cations to H adducts. Experimental evidence of radical cation scavenging by a neutral radical product of radiolysis in the benzene/ethylene/NaZSM5 system was presented. In that case we took advantage of the fact that benzene radical cation is the sole radiolysis product from benzene and ethylene gives ethyl radical as the primary radiolysis product at 77 K (and n-butyl radical as the secondary product at elevated temperatures). This combination of radiolysis products led to efficient quenching of the radical cation signal. This test strongly supports the possiblity of significant charge transfer between different radiolysis products even under static conditions (no diffusion).

One additional observation in the present work deserves interpretation in light of the reasonable expectation of charge transfer between different radiolysis products. Electron transfer from cyclohexenyl radical to the cyclohexene radical cation (exothermic by 1.9 eV in the gas phase) would help explain why the radiolysis/EPR result at 77 K for cyclohexene in NaZSM5 changes from predominantly radical cation to exclusively cyclohexenyl radical as a result of the modest concentration increase from 350 to 500 μmol/g. There is no transition where both species make appreciable contributions to the spectrum. This is understandable if we only observe the species occurring in excess, that is, the surviving fraction of paramagnetic species following the mutual annihilation caused by charge transfer. This also suggests an explanation why the signal due to cyclohexenyl radical in Figure 1b is very weak—much of the product of proton transfer was consumed by charge transfer.

We assert that charge transfer among radiolysis products alone could give rise to the observed variation with adsorbate of the relative yields of H adducts and radical cations in HZSM5. No other competition between these two product channels needs to be invoked. However, this alone does not provide a basis for predicting the relative concentrations of trapped species. Calculation of the ionization potentials for the H adducts allowed a survey to be made of the driving force (ΔIP) for this reaction for different adsorbates (Table 4). While the ΔIP(vertical) for adsorbates that gave little or no radical cation contribution in the radiolysis/EPR experiment (in particular, TMA, 1-methyl-cyclopentene) lie in the upper range of the molecules studied, ΔIP is as large or larger for other molecules, for example, benzene, that gave appreciable yields of trapped radical cations. Furthermore, all of the ΔIP values in Table 4 are equal to or

greater than that for our test case, electron transfer from ethyl radical (and/or *n*-butyl) to benzene radical cation (1.1−1.2 eV).

There is no correlation between the calculated activation energies for H addition and the pattern observed for the H adduct contribution relative to the radical cation. This is consistent with the assertion made above; H addition is not a barrier-controlled reaction.

4.3. Zeolite−Adsorbate Interactions. Consideration, with the aid of quantum calculations, of the fundamental molecular properties of the adsorbates used in this study leads us to the conclusion that matrix−adsorbate interactions play a critical role in determining the outcome of the radiation chemistry. That is, apart from activation energies and exothermicities of electron transfer, etc., what we are missing is the knowledge of how the location, distribution, and specific interactions between the zeolite and adsorbate molecules influence the formation, stability, and chemical reactions of the paramagnetic intermediates.

Not only does the distribution have obvious consequences for charge transfer reactions because of the exponential fall-off of the electron transfer probability with distance, the distribution and location of adsorbate molecules is probably critical for the initial yields of H adducts. Trapped H(D) atoms can be observed in HZSM5 at 77 K;[41] therefore, radiolytic H atoms probably do not diffuse any appreciable distance at 77 K and on this basis the H adduct yield is likely to depend on the adsorbate concentration (observed) and on the location of adsorbate molecules relative to the site of O−H bond scission. The increase in the relative contribution of the H adduct of TME for 170 K radiolysis compared to 77 K radiolysis is probably explained by longer-range reactions of H atoms.

Indeed, the dependence on adsorbate siting relative to O−H bonds might be more subtle. Formation of H adducts could depend on the precise geometry of hydrogen-bonded complexes formed between the zeolite and the adsorbate and the strength of the hydrogen-bonding interaction. These, in turn, depend on the size, the shape, and the relative basicity of the adsorbate.

One of many competitions that decide chemical outcomes in microporous solids is the competition between reactions that occur at a distance (charge transfer) and reactions that require direct contact. This competition depends on the adsorption distribution−not the specific siting of molecules, but the degree of isolation or aggregation of molecules. Characterization of adsorbate distributions in zeolites and other porous solids at low loading is very difficult, and insights from the radiation chemistry of ZSM5 are some of the first direct clues that we have.

If we assume that decay of radical cations in NaZSM5 occurs strictly by ion−molecule reaction, then the observation of the radical cation implies isolation in the zeolite from other reactant molecules. Thus molecules with less than five carbon atoms evidently adsorb with neighbors in close enough proximity to allow facile ion−molecule reaction without diffusive motion. Adsorbates with six or more carbon atoms are adsorbed in a manner that requires diffusive motion before ion−molecule reactions can take place. (This dichotomy is assumed to be reflected also in the average distributions at room temperature, although some condensation may occur upon rapid freezing in liquid nitrogen.)

From other spectroscopic studies of C_6 molecules, such as benzene,[79] cyclohexadienyl radical,[80] and TME[•+],[78] it has been reasonably well established that C_6 molecules occupy the channel intersections of ZSM5 at low loading. Further evidence shows that sorbate−sorbate interactions for adsorbates of this size (specifically for TME and benzene) in ZSM5 are negli-

gible.[19,80,81] Thus one can speculate on the geometric explanation for a change in the adsorption distributions between C_5 and C_6 molecules (typified by the branched and cyclic molecules in this study). That is, while smaller molecules tend to aggregate in the channels and/or intersections, C_6 molecules are preferentially adsorbed at the channel intersections with single occupancy.

If proton transfer does not occur exclusively by the ion−molecule reaction, that is, if proton transfer occurs to the zeolite, then the above reasoning is ambiguous. By the arguments given above, it seems clear that the larger radical cations are only deprotonated by ion−molecule reactions. However, the data in Table 6 show that the relative radical cation acidity increases with decreasing size and we must ask whether proton transfer to the zeolite might occur for the most acidic radical cations. We did not attempt to compute the full energetics of proton transfer from radical cations to the zeolite because this is a much larger task involving treatment of the combined host−guest system. That is, we have not assessed whether proton transfer to the zeolite is feasible in any case. Short of this, however, several observations speak to this question.

We can examine the trend in Table 6 in search of a sharp division between C_5 and C_6. In some cases, the separation is very slight. For example, the calculated values for isobutene, cyclopentene, and cyclohexene differ by less than 2 kcal/mol. The experimental values for isobutene, 1,3-cyclohexadiene, and 1,3,5-cycloheptatriene are equal within 2 kcal/mol. These energy separations are too small to explain the abrupt change from stable radical cation to complete deprotonation, assuming no aggregation and no ion−molecule reaction.

Second, the *n*-hexane radical cation was observed in dilute *n*-hexane/ZSM5 samples.[37] Evaluation of E_{PA} from the literature values of the heats of formation of the *n*-hexane radical cation[53] and *n*-hexyl radical[53,82] gives +179 kcal/mol. From this value we would predict that the *n*-hexane radical cation is more acidic than every radical cation in our study except propene radical cation. Its observation in ZSM5 suggests that the small olefin radical cations would be long-lived also if isolated from other adsorbate molecules.

Finally, ethylene undergoes an ion−molecule reaction in NaZSM5 other than proton transfer, such that no ambiguity exists whether the reaction partner is an adsorbate molecule or the zeolite. Deprotonation of the ethylene radical cation does not even compete with the formation of ethyl radical, despite the ethylene radical cation being more acidic than most other radical cations in our study (Table 6). This is strong evidence that ethylene molecules are not adsorbed homogeneously in NaZSM5, but are aggregated. We conclude that the same is probably true of the other olefins with fewer than six carbons.

5. Conclusions

The radiolysis mechanism that accounts for the data on hydrocarbon radiolysis in ZSM5 can be described by eqs 1−5. The main new addition to the scheme from the present work is the transfer of H atoms from the zeolite to adsorbate molecules. For the molecules studied, this is the only mechanism for H adduct formation, except for ethylene, which undergoes an ion−molecule reaction to form ethyl radical. The scheme does not explicitly treat the reaction of electrons, some of which are trapped by the matrix. The scheme omits other possible radical cation reactions, for example, isomerization and dimerization. For certain alkane radical cations in ZSM5 fragmentation reactions become important.[15] Finally, eqs 1−5 typify the radiolytic processes that occur in other porous silicate matrixes,

Hydrogen Addition to Hydrocarbons in Radiolyzed Zeolites

J. Phys. Chem. B, Vol. 103, No. 43, 1999 **9229**

but geometric and other specific factors can turn a minor process in one matrix into the dominant chemical channel in another matrix, and vice versa.

The scavenging of radical cations by other donor molecules was previously studied by radiolysis of ZSM5 samples containing two adsorbates.[18] New in the present work is the evidence that charge transfer among different radiolysis products can be extensive. The example explored here is the charge transfer reaction between a radical cation and a neutral radical. Such reactions create interference between different chemical channels and can significantly alter the distribution of final radiolysis products.

No model system can capture all of the elements of the radiation chemistry in complex heterogeneous solids; the multiplicity of competing processes that depend on geometric parameters, composition, specific matrix−adsorbate interactions, etc., is too great. Nevertheless, the ZSM5-plus-adsorbate model allows us (1) to enumerate fundamental processes, (2) to investigate the interactions between them, and (3) to devise and test strategies to control them. With respect to complex systems, a comprehensive radiolysis mechanism is not appropriate. Rather, strategies, based on fundamental understanding, to enhance or mitigate specific processes or chemical transformations are needed. It is this goal that motivates study of carefully designed models such as the subject of this paper.

References and Notes

(1) Gray, K. A.; Cleland, M. R. *J. Adv. Oxid. Technol*. **1998**, *3*, 22.

(2) Bolton, J. R.; Valladares, J. E.; Zanin, J. P.; Cooper, W. J.; Nickelsen, M. G.; Kajdi, D. C.; Waite, T. D.; Kurucz, C. N. *J. Adv. Oxid. Technol*. **1998**, *3*, 174.

(3) Galav, V.; Waite, T. D.; Kurucz, C. N.; Cooper, W. *J. Contam. Soils* **1997**, *2*, 295.

(4) Hui, F. Y. C.; Eres, G.; Joy, D. C. *Appl. Phys. Lett*. **1998**, *72*, 341.

(5) Lercel, M. J.; Whelan, C. S.; Craighead, H. G.; Seshadri, K.; Allara, D. L. *J. Vac. Sci. Technol., B* **1996**, *14*, 4085.

(6) Tanenbaum, D. M.; Lo, C. W.; Isaacson, M.; Graighead, H. G.; Rooks, M. J.; Lee, K. Y.; Huang, W. S.; Chang, T. H. P. *J. Vac. Sci. Technol., B* **1996**, *14*, 3829.

(7) Weber, W. J.; Ewing, R. C.; Angell, C. A.; Arnold, G. W.; Cormack, A. N.; Delaye, J. M.; Griscom, D. L.; Hobbs, L. W.; Navrotsky, A.; Price, D. L.; Stoneham, A. M.; Weinberg, M. C. *J. Mater. Res*. **1997**, *12*, 1946.

(8) Corma, A.; Fornes, V.; Garcia, H.; Miranda, M. A.; Primo, J.; Sabater, M.-J. *J. Am. Chem. Soc*. **1994**, *116*, 2276.

(9) Yoon, K. B.; Hubig, S. M.; Kochi, J. K. *J. Phys. Chem*. **1994**, *98*, 3865.

(10) Brancaleon, L.; Brousmiche, D.; Rao, V. J.; Johnston, L. J.; Ramamurthy, V. *J. Am. Chem. Soc*. **1998**, *120*, 4926.

(11) Sun, H.; Blatter, F.; Frei, H. In *Heterogeneous Hydrocarbon Oxidation*; Warren, B. K., Oyama, S. T., Eds.; American Chemical Society: Washington, DC, 1996; p 409.

(12) Pitchumani, K.; Warrier, M.; Ramamurthy, V. *J. Am. Chem. Soc*. **1996**, *118*, 9428.

(13) Qin, X.-Z.; Trifunac, A. D. *J. Phys. Chem*. **1990**, *94*, 4751.

(14) Barnabas, M. V.; Trifunac, A. D. *J. Chem. Soc., Chem. Commun*. **1993**, *813*.

(15) Barnabas, M. V.; Werst, D. W.; Trifunac, A. D. *Chem. Phys. Lett*. **1993**, *204*, 435.

(16) Werst, D. W.; Tartakovsky, E. E.; Piocos, E. A.; Trifunac, A. D. *J. Phys. Chem*. **1994**, *98*, 10249.

(17) Piocos, E. A.; Werst, D. W.; Trifunac, A. D.; Eriksson, L. A. *J. Phys. Chem*. **1996**, *100*, 8408.

(18) Werst, D. W.; Han, P.; Trifunac, A. D. *Chem. Phys. Lett*. **1997**, *269*, 333.

(19) Chemerisov, S. D.; Werst, D. W.; Trifunac, A. D. *Chem. Phys. Lett*. **1998**, *291*, 262.

(20) Werst, D. W.; Trifunac, A. D. *Acc. Chem. Res*. **1998**, *31*, 651.

(21) Werst, D. W.; Trifunac, A. D. *Magn. Reson. Rev*. **1998**, *17*, 163.

(22) Edlund, O.; Kinell, P.-O.; Lund, A.; Shimizu, A. *Adv. Chem. Ser*. **1968**, *82*, 311.

(23) Zhang, G.; Mao, Y.; Thomas, J. K. *J. Phys. Chem. B* **1997**, *101*, 7100.

(24) Piocos, E. A.; Han, P.; Werst, D. W. *J. Phys. Chem*. **1996**, *100*, 7191.

(25) Werst, D. W.; Han, P. *Catal. Lett*. **1997**, *45*, 253.

(26) Shiotani, M.; Lindgren, M. *Mol. Eng*. **1994**, *4*, 179.

(27) Yahiro, H.; Yamaji, K.; Shiotani, M. *Chem. Lett*. **1995**, 601.

(28) Beck, J. S.; Vartuli, J. C.; Roth, W. J.; Leonowicz, M. E.; Kresge, C. T.; Schmitt, K. D.; Chu, C. T.-W.; Olson, D. H.; Shepard, E. W.; McCullen, J. B.; Higgins, J. B.; Schlenker, J. L. *J. Am. Chem. Soc*. **1992**, *114*, 10834.

(29) Meier, W. M.; Olson, D. H.; Baerlocher, Ch. *Zeolites* **1996**, *17*, 1.

(30) Werst, D. W.; Han, P.; Trifunac, A. D. *Radiat. Phys. Chem*. **1998**, *51*, 255.

(31) Werst, D. W.; Piocos, E. A.; Tartakovsky, E. E.; Trifunac, A. D. *Chem. Phys. Lett*. **1994**, *229*, 421.

(32) Shiga, T.; Lund, A. *J. Phys. Chem*. **1973**, *77*, 453.

(33) Fessenden, R. W.; Schuler, R. H. *J. Chem. Phys*. **1963**, *39*, 2147.

(34) Adrian, F. J.; Bowers, V. A.; Cochran, E. L. *J. Chem. Phys*. **1975**, *63*, 919.

(35) McDowell, C. A.; Shimokoshi, K. *J. Chem. Phys*. **1974**, *60*, 1619.

(36) Toriyama, K.; Nunome, K.; Iwasaki, M. *J. Phys. Chem*. **1986**, *90*, 6836.

(37) Toriyama, K.; Nunome, K.; Iwasaki, M. *J. Am. Chem. Soc*. **1987**, *109*, 4496.

(38) Wood, D. E.; McConnell, H. M. *J. Chem. Phys*. **1962**, *37*, 1150.

(39) Faucitano, A.; Buttafava, A.; Martinotti, F. *Radiat. Phys. Chem*. **1995**, *45*, 45.

(40) Adam, W.; Walter, H., Chen, G.-F.; Williams, F. *J. Am. Chem. Soc*. **1992**, *114*, 3007.

(41) Werst, D. W.; Trifunac, A. D.; Choure, S. C. Unpublished results.

(42) Beck, L. W.; Xu, T.; Nicholas, J. B.; Haw, J. F. *J. Am. Chem. Soc*. **1995**, *117*, 11594.

(43) Wichterlova, B.; Novakova, J.; Prasil, Z. *Zeolites* **1988**, *8*, 117.

(44) Becke, A. D. *J. Chem. Phys*. **1993**, *98*, 1372.

(45) Becke, A. D. *J. Chem. Phys*. **1993**, *98*, 5648.

(46) Stephens, P. J.; Devlin, F. J.; Chabalowski, C. F.; Frisch, M. J. *J. Phys. Chem*. **1994**, *98*, 11623.

(47) Krishnan, R.; Binkley, J. S.; Pople, J. A. *J. Chem. Phys*. **1980**, *72*, 650.

(48) McLean, A. D.; Chandler, G. S. *J. Chem. Phys*. **1980**, *72*, 5639.

(49) Frisch, M.; Binkley, J. S.; Pople, J. A. *J. Chem. Phys*. **1984**, *80*, 3265.

(50) Frisch, M. J.; Trucks, G. W.; Schlegel, H. B.; Gill, P. M. W.; Johnson, B. G.; Robb, M. A.; Cheeseman, J. R.; Keith, T. A.; Peterson, G. A.; Montgomery, J. A.; Raghavachari, K.; Al-Laham, M. A.; Zakrzewske, V. G.; Ortiz, J. V.; Foresman, J. B.; Cioslowski, J.; Stefanov, B. B.; Nanayakkara, A.; Challacombe, M.; Peng, C. Y.; Ayala, P. Y.; Chen, W.; Wong, M. W.; Andres, J. L.; Replogle, E. S.; Gompers, R.; Martin, R. L.; Fox, D. J.; Binkley, J. S.; Defrees, D. J.; Baker, J.; Stewart, J. P.; Head-Gordon, M.; Gonzalez, C.; Pople, J. A. Gaussian 94 (Revision E.2); Gaussian Inc.: Pittsburgh, PA, 1995.

(51) Frisch, M. J.; Trucks, G. W.; Schlegel, H. B.; Scuseria, G. E.; Robb, M. A.; Cheeseman, J. R.; Zakrewske, V. G.; Montgomery, J. A.; Stratmann, R. E.; Burant, J. C.; Dapprich, S.; Millam, J. M.; Daniels, A. D.; Kudin, K. N.; Strain, M. C.; Farkas, O.; Tomasi, J.; Barone, V.; Cossi, M.; Cammi, R.; Mennucci, B.; Pomelli, C.; Adamo, C.; Clifford, S.; Octerski, J.; Peterson, G. A.; Ayala, P. Y.; Cui, Q.; Morokuma, K.; Malick, D. K.; Rabuck, A. D.; Raghavachari, K.; Foresman, J. B.; Cioslowski, J.; Ortiz, J. V.; Stevanov, B. B.; Liu, G.; Liashenko, A.; Piskorz, P.; Komaromi, I.; Gomperts, R.; Martin, R. L.; Fox, D. J.; Keith, T.; Al-Laham, M. A.; Peng, C. Y.; Nanayakkara, A.; Gonzalez, C.; Challacombe, M.; Gill, P. M. W.; Johnson, B. G.; Chen, W.; Wong, M. W.; Andres, J. L.; Head-Gordon, M.; Repogle, E. S.; Pople, J. A. Gaussian 98 (Revision A.5); Gaussian Inc.: Pittsburgh, PA, 1998.

(52) Becke, A. D. *J. Chem. Phys*. **1996**, *104*, 1040.

(53) In *Gas Phase and Ion and Neutral Thermochemistry*; Lias, S. G.; Bartmess, J. E.; Liebman, J. F.; Holmes, J. L.; Levin, R. D.; Mallard, W.

G., Eds.; Journal of Physical and Chemical Reference Data, Vol. 17, Supplement No. 1; American Chemical Society: New York, 1988.

(54) Eriksson, L. A. *Mol. Phys*. **1997**, *91*, 827.

(55) Gauld, J. W.; Eriksson, L. A.; Radom, L. *J. Phys. Chem. A* **1997**, *101*, 1352.

(56) Barone, J. L. In *Recent Advances in Density Functional Methods, Part 1*; Chong, D. P., Ed.; World Scientific: Singapore, 1995.

(57) Durant, J. L. *Chem. Phys. Lett*. **1996**, *256*, 595.

(58) Wong, M. W.; Radom, L. *J. Phys. Chem. A* **1998**, *102*, 2237.

(59) Nicovich, J. M.; Ravishankara, A. R. *J. Phys. Chem*. **1984**, *88*, 2534.

(60) Roduner, E.; Bartels, D. M. *Ber. Bunsen-Ges. Phys. Chem*. **1992**, *96*, 1037.

(61) In *CRC Handbook of Chemistry and Physics*; Lide, D. R., Ed.; CRC Press: New York, 1998.

(62) Iwasaki, M.; Toriyama, K.; Muto, H.; Nunome, K.; Fukaya, M. *J. Phys. Chem*. **1981**, *85*, 1326.

(63) Muto, H.; Toriyama, K.; Nunome, K.; Iwasaki, M. *Radiat. Phys. Chem*. **1982**, *19*, 201.

(64) Iwasaki, M.; Toriyama, K.; Nunome, K.; Fukaya, M.; Muto, H. *J. Phys. Chem*. **1977**, *14*, 1410.

(65) Iwasaki, M.; Muto, H.; Toriyama, K.; Fukaya, M.; Nunome, K. *J. Phys. Chem*. **1979**, *83*, 1590.

(66) Shkrob, I. A.; Trifunac, A. D. *J. Chem. Phys*. **1997**, *107*, 2374.

(67) Wong, P. K. *J. Phys. Chem*. **1971**, *75*, 201.

(68) Shinohara, H.; Sato, H.; Washida, N. *J. Phys. Chem*. **1990**, *94*, 6718.

(69) Zhong, Q.; Poth, Z. Shi; Ford, J. V.; Castleman, A. W., Jr. *J. Phys. Chem. B* **1997**, *101*, 4203.

(70) Ohnishi, S.-I.; Tanei, T.; Nitta, I. *J. Chem. Phys*. **1962**, *37*, 2402.

(71) Shida, T.; Hanazaki, I. *Bull. Chem. Soc. Jap*. **1970**, *43*, 646.

(72) Trace amounts of H adduct in some NaZSM5 samples, for example, as reported for TME [ref 16], might be accounted for by radiolysis of silanols at lattice defects and/or bridging hydroxyls left over from incomplete ion exchange.

(73) Shiotani, M. *Magn. Reson. Rev*. **1987**, *12*, 333.

(74) Williams, F.; Qin, X.-Z. *Radiat. Phys. Chem*. **1988**, *32*, 299.

(75) Fujisawa, J.; Sato, S.; Shimokoshi, K.; Shida, T. *J. Phys. Chem*. **1985**, *89*, 5481.

(76) In line with the present discussion, a revision of the previous interpretation [ref 31] of the ionization of 1,3,5-cycloheptatriene in NaZSM5 is in order. The partial decay of the radical cation in NaZSM5 at 77 K is probably due to an anomalous adsorption distribution caused by the near exclusion of a molecule this size from the ZSM5 channels. It was found that trapping of the radical cation was less successful for increasing Al (Na$^+$) concentrations, which is consistent with hindrance of diffusion by the extraframework cations. (For evidence of the hindering effect of sodium ions on diffusion in ZSM5, see ref 77.).

(77) Kustanovich, I.; Vieth, H. M.; Luz, Z.; Vega, S. *J. Phys. Chem*. **1989**, *93*, 7427.

(78) Roduner, E.; Crockett, R.; Wu, L.-M. *J. Chem. Soc., Faraday Trans*. **1993**, *89*, 2101.

(79) Mentzen, B. F.; Lefebvre, F. *Mater. Res. Bull*. **1997**, *32*, 813.

(80) Roduner, E.; Stolmar, M.; Dilger, H.; Reid, I. D. *J. Phys. Chem*. **1998**, *102*, 7591.

(81) Ashtekar, S.; Hastings, J. J.; Gladden, L. F. *J. Chem. Soc., Faraday Trans*. **1998**, *94*, 1157.

(82) Cohen, N. *J. Phys. Chem*. **1992**, *96*, 9052.